Reliability Engineering and System Safety 175 (2018) 105–118

Contents lists available at ScienceDirect

Reliability Engineering and System Safety

journal homepage: www.elsevier.com/locate/ress

A traffic-responsive signal control to enhance road network resilience with hazmat transportation in multiple periods

Suh-Wen Chiou

Department of Information Management, National Dong Hwa University, Taiwan

ARTICLE INFO

Keywords:
Traffic-responsive signal control
Linked traffic signal
Hazardous materials transportation
Road network resilience
Mathematical optimization model
Multi-period of travel demands

ABSTRACT

To enhance resilience of urban road networks, a flexible signal control is proposed to mitigate period-dependent travel delay and random risk associated with hazardous materials (hazmat) transportation. A mathematical optimization model is presented to find period-dependent traffic responsive signal control subject to equilibrium traffic assignments. In the presence of hazmat transportation, a set of scenarios for uncertain exposure risk on links is investigated. A two-stage new solution scheme is proposed to solve a traffic responsive signal control in multiple periods. In order to demonstrate robustness of period-dependent signal control for hazmat transportation, numerical computations using realistic road network are made with recently proposed ones. These results reported obviously indicate that proposed period-dependent signal control can be more resilient than existing ones against a high-consequence of exposure risk in the presence of hazmat transportation.

1. Introduction

For urban road network with signalized junctions, most travel delay depends on correct and continuous operation of linked traffic signals at junctions. The internal complexity of traffic signal control in area wide road networks and their reliance on other linked signals can operate in conjunction to amplify the negative impacts of traffic flows [1]. The reliability of linked traffic signal controls is accordingly dependent on structural and functional robustness of interdependent signal-controlled junctions. By offering an insightful measure of network robustness, for example, Bell [2] developed a novel game-theoretic model that leverages the ranking of all links according to the effect of their failure on damaging the network performance, and allows the attacker to fail one link at a time in order to maximize the expected trip cost. Zhang and Mahadevan [3] extended [2] but took a probabilistic solution discovery algorithm to multiple failure scenarios. Fang and Sansavini [4], Ding et al. [5] respectively proposed tri-level optimization model to make decisions for power grid protection. To make better protection for network robustness against uncertainty, Ding et al. [5] proposed a two-stage robust optimization and solved by column-and-constraints generation algorithm with a master and sub-problem framework. A resilience induced network design to quantify robustness for critical infrastructure system has also received increasing attention [6–10] more recently. For example, Zio [9] provides a systematic view on the problem of vulnerability and risk of critical infrastructures with emphasis on its relationship to protection and resilience in practice. In order to understand the technical meanings and foundation of resilience, Woods [11] proposes four aspects of concept about resilience and its implications for applications in real world. Barker et al. [7] proposed indicators to quantify adverse impact on system resilience in the presence of disruptions. The most affected component can be identified and the importance of system component can be measured. As for the resilience of transportation system, Chen and Miller-Hooks [6] presented an indicator of network resilience that quantifies the ability of an intermodal freight transport network to recover from disruptions. Considering inherent coping ability of an intermodal freight transport network, the proposed resilience accounting for the impact of possible recovery decisions undertaken can mitigate negative consequences of disruptions and meet desired operational target within budget requirement. A mixed integer mathematical program is presented and solved with classical methods. Zhang et al. [10] proposed a resilience-based network design optimization problem. Consider a key characteristic of resilience as the ability of restoring functionality and performance in response to a disruptive event. Zhang et al. [10] proposed a non-linear restoration function to consider the remaining capacity, the degree to which capability can be recovered during a desirable time horizon, and the recovery speed. In order to minimize cost, a pre-determined resilience constraint which requires that the system performance spring back to a desired level after the disruptive event is proposed. A novel probabilistic solution is also proposed with numerical examples to demonstrate efficiency of proposed approach.

A hazmat transportation network design problem has long been deemed one most challenging issue [12–14] facing transportation policy decision makers. Due to imminent exposure risk associated with the

E-mail address: chiou@mail.ndhu.edu.tw

https://doi.org/10.1016/j.ress.2018.03.016
Received 12 June 2017; Received in revised form 1 March 2018; Accepted 7 March 2018
Available online 13 March 2018
0951-8320/

accidental release of hazmat, the people living and working around the roads heavily used for hazmat transportation inevitably incur most of the risk during transportation. For urban road network with hazmat transportation, it is of paramount importance for decision makers to determine a flexible signal control to mitigate travel delay and reduce transportation risk of goods and people. In order to effectively decrease traffic delay for all road users and reduce travel risk in the presence of hazmat transportation, these connected signal controlled junctions in urban cities can be regarded as critical infrastructures (CIs) [15,16]. Assuming availability of statistics for hazmat risk and probability, many risk models have been proposed such as the maximum risk model [13], the mean-variance risk model [13], and a value-at-Risk (VaR) [14] with application to hazmat routing and shipments. Recognizing the fact that hazmat accidents are low-probability high-consequence events, for example, Toumazis and Kwon [12] proposed a conditional VaR risk measure on time-dependent vehicular networks where the accident probabilities and accident consequences are time-dependent. To deal with the robustness of solutions for hazmat network design with linear delay, various heuristics were presented. For example, supposing that hazmat traffic also belongs to regular traffic flow, Wang et al. [17] proposed a duration-population-frequency risk measure of hazmat exposure in road network. A hazmat network design can be formulated as a mathematical program with equilibrium constraints where dual tolls are set respectively for regular traffic and hazmat carriers. Following Wardrop' first principle, the toll-user equilibrium for regular traffic can be formulated as a variational inequality.

Consider the concept of resilience to measure not only the system's ability to absorb perturbations, but also its ability to rapidly recover from perturbations. Adjetey-Bahun et al. [18] proposed a simulation-based model to quantify resilience of mass railway transportation systems. The resilience of mass railway systems can be measured by quantifying passenger delay and passenger load as the system's performance indicators. Considering whether a traffic network is able to sustain and respond to disruption when a disruptive event takes place, Nogal et al. [19] proposed a model to quantify the resilience of a traffic network. A dynamic equilibrium-restricted assignment is proposed to identify traffic network weakness, and to analyse the effect of user knowledge about the traffic network state. Additionally, in order to assess the resilience of a traffic network when a given perturbation occurs, the proposed model accounts for the system impedance to alter its previous state, given that the actual capacity of adaption of the system to the new situations determines users' behaviour. More recently, Fotouhi et al. [8] proposed a traffic and electric power system to quantify the resilience of a coupled system under possible multiple hazards. In order to quantify the resilience of the traffic network, equilibrium route choice for road users at signalized road network is considered. The travel delay incurred by users due to potential recovery actions taken can be estimated accordingly.

Consider urban road networks with signal-controlled junctions. Few of flexible signal controls have been proposed to enhance robustness of traffic road networks under uncertainty except from [20–25]. For instance, Ukkusuri et al. [21] proposed a robust signal control using mean-variance model (MSR) to find system optimum under uncertain travel demand. Taking account of traffic dynamics and using a macroscopic traffic flow model to capture vehicular movement within urban road network, Ukkusuri et al. [21] proposed a mathematical program for a dynamic signal control. While focusing on how road traffic moves in each road segment during each time increment, the proposed MSR can be practically restrictive due to highly intensive computations. Zhang et al. [22] proposed a robust signal control for coordinated signal design along arterials in urban road networks. A scenario-based stochastic programming model is proposed to optimize the timings of coordinated signal control under day-to-day travel demand variation. A simulation-based generic algorithm is used to find optimal common cycle time, green splits, and offsets that minimize the expected delay incurred by high-consequence demand scenarios. Again, due to intensive computational overheads, the proposed signals can be only applied to road networks of small scale in practice. In order to determine a robust signal control that is resilient for any realization of uncertain travel demand, moreover, Yin [24] proposed a set-based robust signal control (SR) for isolated junctions. A norm-bounded model using a likelihood region that confines traffic arrivals at downstream signal-controlled junctions is proposed to determine robust signal control. Li [25] continues to propose a discretization model and finds good solutions by dynamic programming algorithms. However, due to restriction of traffic flow in a predetermined likelihood region of travel demand, the solutions of SR seem to be rather conservative for a general road network against high consequence of uncertainty. More recently, Tong et al. [23] presented a stochastic programming model to effectively schedule multi-period signal timing plans (MSP) that minimize the expected vehicle delay for oversaturated signal-controlled junctions. As it was reported, MSP achieved better results in vehicle delay, total throughput, and vehicle queue lengths than those did the deterministic one for uncertain traffic flows. Considering adaptability of traffic signal control under hazmat transportation, the author [20] proposed a risk-averse signal control (ER) to mitigate imminent risk of hazmat transportation in single periods. Although ER exhibited computational advantage of robustness against the worst case of travel demand, it was incurred a relatively high optimality loss as the level of uncertainty of demand in subsequent periods increases. As it was reported, the efficiency of ER to mitigate uncertain travel demand in single periods can be inevitably undermined due to growing optimality loss when level of uncertainty in travel demand is in a steady increase.

While these recently proposed signal controls provide methods to mitigate total travel delay for all road users both at isolated signal-controlled junctions and in area wide signalized road networks, none considers increasing resilience of linked signals with growing OD travel demands in multiple periods. This paper takes a step toward filling this gap. In most urban road networks with linked signals, cascading travel delay in multiple periods can be incurred by regular road users due to protracted congestion. Specifically, regular road users can incur prolonged travel delay as a result of potential vulnerability of link capacity loss in the presence of hazmat transportation. For hazmat carriers, major protracted travel delay along chosen routes can be also explicitly affected by the volume of regular traffic flows in multiple periods at downstream signalized junctions. In order to effectively mitigate period-dependent travel delay and enhance resilience of road traffic network with linked signals for multi-period OD flows, these linked traffic-responsive signals can be regarded as part of period-dependent CI of road traffic network for OD flow in multiple periods. A period-dependent traffic-responsive signal control can be proposed in this paper for the following purposes. First, to enhance current resilience of CI with linked signals, a traffic-responsive signal control quantifies period-dependent performance index for OD flows in multiple periods. Next, a systematic assessment is performed to improve robustness of road traffic network with linked signals through taking account of both regular road users' and hazmat carriers' response to period-dependent signal controls in multiple periods. Additionally, in this paper, a mathematical model is presented to evaluate how traffic-responsive signal control and hazmat risk interact to influence the expected performance of traffic delay and transportation risk in multiple periods. To effectively mitigate fragility of traffic-responsive signal control in multiple periods while accounting for regular traffic and hazmat carriers' response, a mathematical program with equilibrium constraints (MPEC) is proposed. A flexible signal control (FLS) for multi-period travel demand is presented to enhance resilience of signalized road network against high consequence of imminent exposure risk for hazmat transportation. Due to non-linearity of equilibrium constraints, a two-stage new solution method for MPEC is presented. To demonstrate the effectiveness and computational feasibility of proposed traffic-responsive signal control for OD flows in multiple periods, numerical computations and comparisons are made with existing signal controls. These results reported obviously indicate that

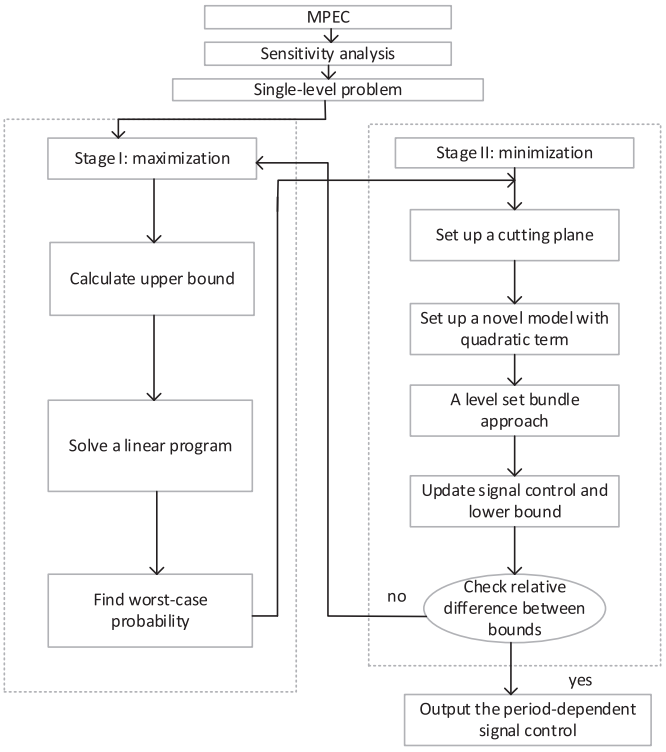

Fig. 1. A two-stage solution structure.

proposed FLS can be more resilient than did those existing ones against a high-consequence of exposure risk in the presence of hazmat transportation.

The contribution made from this paper in the literature can be summarized as follows.

(1) A period-dependent traffic-responsive signal control to quantify resilience of road network in the presence of hazmat transportation is proposed for OD travel demands in multiple periods. A bi-objective performance index for linked signals is presented through a pre-determined parameter between period-dependent traffic queues [20] and risk measure [17]. Period-dependent adaptability for linked signal control is derived not only from the taking of proactive actions in signal settings but also from period-dependent route choices that are sustained following users' equilibrium between regular road users and hazmat carriers. The interdependency of period-dependent linked signals can be regarded as part CI in area wide road traffic networks. The resilience of CI can be estimated by linear combination of period-dependent traffic queues at downstream signalized junctions and duration-population-frequency risk measure in the presence of hazmat carriers. Period-dependent interdependencies arising from the need for estimating period-dependent traffic delay incurred at downstream linked signals between regular traffic users and hazmat carriers are taken into account. Furthermore, contrary to earlier work in quantifying resilience of road network like [8,10] where inherent uncertainties are assumed as a priori, in this paper a period-dependent min-max scenario-based model is presented. Accordingly, a two-stage robust model is proposed to highlight the resilience of CI of area wide linked traffic control in the worst-case scenario.

(2) A mathematical program with equilibrium constraints (MPEC) is first proposed while accounting for period-dependent route choices between regular road users and hazmat carriers in multi-period OD travel demands. Due to non-linearity of these equilibrium constraints, a two-stage new solution method is presented as shown in Fig. 1. In order to effectively solve MPEC with uncertain risk in the presence of hazmat transportation, numerical computations and comparisons using example road network and real-data road networks are empirically made with existing signal controls in multiple periods. These results reported obviously indicate that proposed flexible signal control can be more resilient than existing ones against a high-consequence of exposure risk in the presence of hazmat transportation.

The rest of the paper is organized as follows. Section 2 presents period-dependent equilibrium traffic assignments respectively for regular traffic users and hazmat carriers. Section 3 presents a new mathematical program with equilibrium constraints in the presence of random risk associated with hazmat transportation. The period-dependent performance measure for linked signal controlled road network can be quantified by a bi-objective through a pre-determined parameter. Due to non-convexity of mathematical optimization model, in Section 4, a two-stage new solution algorithm is presented to effectively determine a resilient linked signal control. To demonstrate effectiveness and computational feasibility of proposed signal control against uncertain risk, in Section 5, numerical computations and comparisons are made with recently proposed ones. Conclusions and discussions of this paper are summarized in Section 6 together with sensitivity analysis for mathematical model in Appendix.

2. Period-dependent equilibrium for scenario-based set of uncertainty

To effectively cope with period-dependent travel delay incurred by regular users and hazmat carriers under imminent exposure risk of hazards, in this section, a period-dependent equilibrium assignment for regular traffic and hazmat carriers are respectively proposed. In order to quantify resilience of linked signal controlled road network in the presence of hazmat carriers, a period-dependent duration-population-frequency risk measure is used following earlier work of [17] for hazmat carriers' equilibrium assignment. Notation used throughout this paper is presented first.

2.1. Notation

Let $G(N, L)$ denote a directed road network, where N represents a set of signal controlled junctions and L represents a set of links denoted by a, $\forall a \in L$. Each traffic stream approaching any junction is represented by its own link.

W - a set of origin-destination (OD) pairs.
W^H - a set of OD pairs for hazmat transportation.
R_i - a set of routes between OD pair i, $\forall i \in W \cup W^H$.
$T = \{t_i, i = 1, 2, ..\}$ - a set of multiple time periods.
$Q = [Q_i^t]$ - the matrix of period-dependent regular traffic demands for OD pair i within some time period t,$\forall t \in T$, $\forall i \in W$.
$q = [q_i^t]$ - the matrix of period-dependent hazmat transportation travel demands for OD pair i within some time period t, $\forall t \in T$, $\forall i \in W^H$.
ζ^t - the reciprocal of period-dependent common cycle time for some time period t, $\forall t \in T$.
$\zeta_{\min}$, $\zeta_{\max}$ - the minimum and maximum reciprocal of the common cycle time.
$\theta^t = [\theta_{jm}^t]$ - the vector of period-dependent start of green for various links within some time period t, $\forall t \in T$ as proportions of cycle time where θ_{jm}^t is start of next green for signal group j at junction m.
$\phi^t = [\phi_{jm}^t]$ - the vector of period-dependent duration of green for various links within some time period t, $\forall t \in T$ as proportions of cycle time where ϕ_{jm}^t is the duration of green for signal group j at junction m.
τ_{ijm}^t - the period-dependent clearance time for some time period t, $\forall t \in T$ between the end of green for signal group i and the start of green for incompatible signal group j at junction m.

$\Psi^t = (\zeta^t, \theta^t, \phi^t)$ - the set of period-dependent signal setting variables for some time period t, $\forall t \in T$, respectively for the reciprocal of common cycle time, start and duration of greens.

$\Omega_m^t(i,j)$ - period-dependent collection of numbers 0 and 1 for each pair of incompatible signal groups at junction m for some time period t, $\forall t \in T$, where $\Omega_m^t(i,j) = 0$ if the start of green for signal group i precedes that of j and 1, otherwise.

g_a^t - duration of period-dependent effective green for link a, $\forall a \in L$ within some time period t, $\forall t \in T$.

$g_{\min}$ - the minimum green.

ρ_a - maximum degree of saturation for link a, $\forall a \in L$.

s_a^t - period-dependent saturation flow on link a for some time period t, $\forall t \in T$, $\forall a \in L$.

D_a^t - the rate of period-dependent delay on link a for some time period t, $\forall t \in T$, $\forall a \in L$.

S_a^t - the number of period-dependent stops per unit time on link a for some time period t,$\forall t \in T$, $\forall a \in L$.

$\bar{r}^t = [\bar{r}_a^t]$ - the vector of period-dependent nominal risk of accidental release of hazmat on link a for some time period t, $\forall t \in T$, $\forall a \in L$.

$\hat{r}^t = [\hat{r}_a^t]$ - the vector of period-dependent step-length risk of accidental release of hazmat on link a for some time period t, $\forall t \in T$, $\forall a \in L$.

$r^{s,t} = [r_a^{s,t}]$ - the vector of scenario-based risk of accidental release of hazmat on link a for some time period t, such that $r_a^{s,t} \in [\bar{r}_a^t, \bar{r}_a^t + \hat{r}_a^t]$, $\forall t \in T$,$\forall a, s \in L$.

Γ^t - period-dependent budget of all uncertain link risk $r^{s,t}$ in all scenarios for some time period t, $\forall s \in L$,$\forall t \in T$.

$p_a^{s,t}$ - a scenario-based incidental probability of accidental release of hazmat on link a for some time period t, $\forall t \in T$, $\forall a, s \in L$.

W_D - weighting factor for rate of delay.

W_S - weighting factor for number of stops.

M_D - monetary factor associated with period-dependent rate of delay D_a^t, $\forall a \in L$, $\forall t \in T$.

M_S - monetary factor associated with period-dependent stop S_a^t, $\forall a \in L$, $\forall t \in T$.

M_r - monetary factor associated with duration-population-frequency risk measure.

f_a^t - period-dependent regular traffic on link a for some time period t, $\forall t \in T$, $\forall a \in L$.

x_a^t - period-dependent hazmat traffic on link a for some time period t, $\forall t \in T$, $\forall a \in L$.

h_k^t - period-dependent general traffic flow on path k between OD pairs for some time period t, $\forall t \in T$, $\forall k \in \bigcup_{i \in W \cup W^H} R_i$.

λ - link-path incidence matrix with entry $\lambda_{ak} = 1$ if path k uses link a, and 0 otherwise, $\forall a \in L$, $\forall k \in \bigcup_{i \in W \cup W^H} R_i$.

Λ - OD-path incidence matrix with entry $\Lambda_{ik} = 1$ if path k connects OD pair i, and 0 otherwise, $\forall k \in \bigcup_{i \in W \cup W^H} R_i$.

c_a^t - period-dependent travel time on link a for some time period t, $\forall t \in T$, $\forall a \in L$.

$c_{a,0}^t$ - period-dependent un-delayed travel time on link a for some time period t, $\forall t \in T$, $\forall a \in L$.

d_a^t - period-dependent average delay on link a for some time period t, $\forall t \in T$, $\forall a \in L$.

C_k^t - period-dependent travel time on path k for some time period t, $\forall t \in T$, $\forall k \in \bigcup_{i \in W \cup W^H} R_i$.

2.2. Period-dependent equilibrium assignment for regular traffic flow

For every time period t, $\forall t \in T$, a period-dependent travel time can be calculated as a sum of un-delayed travel time $c_{a,0}^t$, and a period-dependent signal delay d_a^t at downstream signal-controlled junction.

$$c_a^t(\Psi^t, f_a^t) = c_{a,0}^t + d_a^t(\Psi^t, f_a^t), \ \forall t \in T \tag{1}$$

According to Wardrop's first principle, a period-dependent equilibrium assignment can be represented for regular traffic with multi-period travel demand. Suppose that period-dependent signal delay at downstream junction is mainly dependent on the amount of regular traffic, a period-dependent user equilibrium traffic flow f^t for multi-period travel demand Q^t, $\forall t \in T$can be determined.

$$\begin{aligned} \underset{f_a^t(\Psi^t)}{Min} \ & \sum_{a \in L} \int_0^{f_a^t(\Psi^t)} c_a^t(\Psi^t, w) dw \\ subject\ to \ & \sum_{k \in R_i} h_k^t = Q_i^t, \forall i \in W \\ & f_a^t = \sum_{k \in \bigcup_{i \in W} R_i} \lambda_{ak} h_k^t \ \ \forall a \in L \\ & h_k^t \geq 0, \forall k \in \bigcup_{i \in W} R_i \end{aligned} \tag{2}$$

A period-dependent user equilibrium flow in (2) can be also identified by a variational inequality [26,27]. Let Φ^t denote a feasible set for period-dependent traffic flow f^t for a multi-period travel demand Q^t such that

$$\Phi^t = \{ f^t : f^t = \lambda h^t, \Lambda h^t = Q^t, h^t \geq 0 \}, \ \forall t \in T \tag{3}$$

A period-dependent user equilibrium traffic flow f^t for a multi-period travel demand Q^t, $\forall t \in T$ can be determined for every $\tilde{f} \in \Phi^t$.

$$c^t(\Psi^t, f^t)(\tilde{f} - f^t(\Psi^t)) \geq 0, \ \forall t \in T \tag{4}$$

The solution set for (3) can be denoted by $\Omega^t(\Psi^t)$.

2.3. A period-dependent scenario-based equilibrium for hazmat carriers

For period-dependent hazmat traffic a scenario-based equilibrium assignment can be presented as follows. Let $z_a^{s,t}$ denote a scaled deviation for random link risk r in some realization scenario s, $\forall t \in T$, $\forall a, s \in L$. It is assumed that a scenario-based link risk $r_a^{s,t}$ for some time period t, $\forall t \in T$, lies in a polyhedron $[\bar{r}_a^t, \bar{r}_a^t + \hat{r}_a^t]$ within a budget Γ^t such that

$$r_a^{s,t} = \bar{r}_a^t + z_a^{s,t} \hat{r}_a^t, \ \forall a \in L \tag{5}$$

with

$$\sum_{a,s \in L} z_a^{s,t} \leq \Gamma^t; \ z_a^{s,t} \in \{0,1\}, \forall t \in T, \forall a, s \in L \tag{6}$$

According to [17], for every scenario s, $\forall s \in L$, a period-dependent duration-population-frequency risk measure is used in the following way.

$$c_a^t(\Psi^t, f_a^t) r_a^{s,t} x_a^{s,t}, \ \forall t \in T, \ \forall a \in L \tag{7}$$

Thus, for every time period t, $\forall t \in T$ a scenario-based equilibrium assignment for hazmat carriers can be presented. For every scenario s, $\forall s \in L$, it is to find a scenario-based hazmat flow $x_a^{s,t}$ such that $x_a^{s,t}$, $\forall a \in L$, solves the following minimization.

$$\begin{aligned} \underset{x_a^{s,t}(\Psi^t)}{Min} \ & \sum_{a \in L} \int_0^{x_a^{s,t}(\Psi^t)} c_a^t(\Psi^t, f_a^t) r_a^{s,t} dw \\ subject\ to \ & \sum_{k \in R_i} h_k^t = q_i^t, \forall i \in W^H \\ & x_a^{s,t} = \sum_{k \in \bigcup_{i \in W^H} R_i} \lambda_{ak} h_k^t, \ \forall a, s \in L \\ & h_k^t \geq 0, \forall k \in \bigcup_{i \in W^H} R_i \end{aligned} \tag{8}$$

A period-dependent equilibrium flow in (8) can be analogously identified by a variational inequality. Let $\tilde{\Phi}^t$ denote a feasible set for period-dependent hazmat traffic x^t with a multi-period travel demand q^t such that

$$\tilde{\Phi}^t = \{ x^t : x^t = \lambda h^t, \Lambda h^t = q^t, h^t \geq 0 \}, \ \forall t \in T \tag{9}$$

A variational inequality for (8) can be presented if and only if the gradient of objective function for (8) is available. It turns out that a scenario-based duration-population-frequency risk measure for period-dependent hazmat carriers in (8) can be expressed as

$$\tilde{c}^{s,t}(\Psi^t, f^t) = c^t(\Psi^t, f^t) r^{s,t},\ \forall t \in T,\ \forall s \in L \tag{10}$$

Similarly, for every time period t, $\forall t \in T$ a period-dependent equilibrium assignment for hazmat carriers can be expressed as a variational inequality. For every scenario s, $\forall s \in L$, it is to find a hazmat flow $x^{s,t}$ for a multi-period travel demand q^t such that for every $\tilde{x} \in \tilde{\Phi}^t$ the inequality holds.

$$\tilde{c}^{s,t}(\Psi^t, f^t)(\tilde{x} - x^{s,t}(\Psi^t)) \geq 0,\ \forall t \in T\ \forall s \in L \tag{11}$$

The solution set for (11) can be denoted by $\tilde{\Omega}^{s,t}(\Psi^t)$, $\forall s \in L$.

3. A flexible signal control

A flexible signal control (FLS) with scenario-based link risk in the presence of hazmat transportation for multi-period travel demand can be formulated as a mathematical program with equilibrium constraints.

3.1. A mathematical program with equilibrium constraints (MPEC)

For every time period t, $\forall t \in T$ a period-dependent constraint set Π^t for signal-controlled road network can be represented as follows. First, for every period t, $\forall t \in T$ a period-dependent cycle time constraint can be expressed as

$$\zeta_{\min} \leq \zeta^t \leq \zeta_{\max} \tag{12}$$

For each signal controlled junction m, the period-dependent phase j green time for all signal groups at junction m can be expressed as

$$g_{\min}\zeta^t \leq \phi^t_{jm} \leq 1, \forall j, m \tag{13}$$

The period-dependent link capacity for all links leading to junction m can be expressed as

$$f^t_a \leq \rho_a s^t_a g^t_a, \forall a \in L \tag{14}$$

and the period-dependent clearance time τ^t_{ijm} for incompatible signal groups i and j at junction m can be expressed as

$$\theta^t_{im} + \phi^t_{im} + \tau^t_{ijm}\zeta^t \leq \theta^t_{jm} + \Omega^t_m(i,j), \quad \forall i, j, m \tag{15}$$

In order to quantify the resilience of period-dependent linked signal controlled road network, a bi-objective performance measure accounting for period-dependent traffic queues [28] and period-dependent risk measure [17] through a pre-determined parameter can be considered as follows. A period-dependent performance index (PI), P^t_0 for regular traffic flow with hazmat carriers can be taken as a weighted sum of a linear combination of the rate of period-dependent delay and the number of period-dependent stop per unit time for each link, and a probabilistic duration-population-frequency risk measure imposed by hazmat carriers with a weighting parameter α, $\alpha \in [0, 1]$.

Introduce a period-dependent incidental probability of accidental release of hazmat on link a, $p^{s,t}_a$ with $\sum_{s\in L} p^{s,t}_a = 1, \forall a \in L, \forall t \in T$ such that

$$\begin{aligned}(1-\alpha)&\sum_{a\in L}\left(D^t_a(\Psi^t, f^t_a)W_D M_D + S^t_a(\Psi^t, f^t_a)W_S M_S\right)\\ &+\alpha\sum_{a,s\in L} c^t_a r^{s,t}_a x^{s,t}_a p^{s,t}_a M_r, \forall t \in T\end{aligned} \tag{16}$$

A period-dependent traffic-responsive signal control for regular traffic flow and hazmat carriers with scenario-based risk measure in multiple periods can be determined by a following mathematical program with equilibrium constraints (MPEC). Recall signal setting $\Psi^t = (\zeta^t, \theta^t, \phi^t)$, it implies

$$\begin{aligned}\underset{\Psi^t, f^t, x^t}{Min}\ \underset{p^t}{Max}\ &\sum_{t\in T} P^t_0(\Psi^t, f^t, x^t, p^t)\\ subject\ to\ &\zeta_{\min} \leq \zeta^t \leq \zeta_{\max}\\ &g_{\min}\zeta^t \leq \phi^t_{jm} \leq 1, \forall j, m\\ &f^t_a \leq \rho_a s^t_a g^t_a, \forall a \in L\\ &\theta^t_{im} + \phi^t_{im} + \tau^t_{ijm}\zeta^t \leq \theta^t_{jm} + \Omega^t_m(i,j), \quad \forall i, j, m\\ &\sum_{s\in L} p^{s,t}_a = 1, \forall a \in L, \forall t \in T\end{aligned} \tag{17}$$

and for all

$$\begin{pmatrix} f' \in \Phi^t \\ x' \in \tilde{\Phi}^t \end{pmatrix},\ \begin{pmatrix} f^t \in \Phi^t \\ x^{s,t} \in \tilde{\Phi}^t, \forall s \end{pmatrix}$$

solves

$$\begin{pmatrix} c^t(\Psi^t, f^t)(f' - f^t(\Psi^t)) \geq 0 \\ \tilde{c}^{s,t}(\Psi^t, f^t)(x' - x^{s,t}(\Psi^t)) \geq 0, \forall s \end{pmatrix}$$

According to sensitivity for PI in (17) (in Appendix), the MPEC (17) can be re-expressed as a following single-level problem.

$$\begin{aligned}\underset{\Psi^t\in\Pi^t}{Min}\ \underset{p^t}{Max}\ &\sum_{t\in T} P^t_1(\Psi^t, p^t)\\ subject\ to\ &\sum_{s\in L} p^{s,t} = 1, \forall t \in T\end{aligned} \tag{18}$$

4. A new solution method

For each period t, the MPEC in (18) can be solved by a following period-dependent min-max model with solutions (Ψ^{t*}, p^{t*}). Let

$$\breve{P}^t = \breve{P}^t(p^t) = \underset{\Psi^t\in\Pi^t}{Min} P^t_1(\Psi^t, p^t) \tag{19}$$

and

$$\hat{P}^t = \hat{P}^t(\Psi^t) = \underset{0\leq p^t\leq 1}{Max} P^t_1(\Psi^t, p^t) \tag{20}$$

To find period-dependent solutions (Ψ^{t*}, p^{t*}) in (19) and (20) such that

$$p^{t*} = Arg\ \underset{0\leq p^t\leq 1}{Max}\ \breve{P}^t(p^t) \tag{21}$$

and

$$\Psi^{t*} = Arg\ \underset{\Psi^t\in\Pi^t}{Min}\ \hat{P}^t(\Psi^t) \tag{22}$$

when the following condition holds:

$$\breve{P}^t \leq \breve{P}^{t*} = \hat{P}^{t*} \leq \hat{P}^t \tag{23}$$

4.1. Linear programming for maximization

An effective upper bound (20) for MPEC (18) can be determined by a following linear maximization with α, $\alpha \in [0, 1]$ for every period t, $\forall t \in T$.

$$\begin{aligned}\hat{P}^t(\Psi^t) = \underset{p^t}{Max}&(1-\alpha)\left(\sum_{a\in L} D^t_a(\Psi^t)W_D M_D + S^t_a(\Psi^t)W_S M_S\right)\\ &+\alpha\sum_{a,s\in L} c^t_a r^{s,t}_a x^{s,t}_a p^{s,t}_a M_r\\ subject\ to\ &\sum_{s\in L} p^{s,t} = 1, \forall t \in T\end{aligned} \tag{24}$$

4.2. A period-dependent approach for minimization

Simialrly, an effective lower bound (19) for every period t, $\forall t \in T$ can be determined by a minimization with α, $\alpha \in [0, 1]$.

$$\breve{P}^{t}(p^t) = \underset{\Psi^t\in\Pi^t}{Min}(1-\alpha)\left(\sum_{a\in L} D_a^t(\Psi^t)W_D M_D + S_a^t(\Psi^t)W_S M_S\right) + \alpha \sum_{a,s\in L} c_a^t r_a^{s,t} x_a^{s,t} p_a^{s,t} M_r \tag{25}$$

According to (24), it implies

$$\breve{P}^{t}(p^t) = \underset{\Psi^t\in\Pi^t}{Min}\hat{P}^{t}(\Psi^t) \tag{26}$$

Moreover, according to Proposition A.2, it implies

$$\partial\hat{P}^{t} = co\left\{\lim_{k\to\infty}\nabla\hat{P}^{t,k} : \Psi^{t,k}\to\Psi^{t*}, \nabla\hat{P}^{t,k} \; exists\right\}, \forall t\in T \tag{27}$$

For period-dependent PI in (26), a linear approximation of $\hat{P}^{t}$ at period-dependent signal setting $\Psi^{t,k}$ along a perturbed direction $\Delta\Psi^{t,k}$ can be established using a bundle of period-dependent gradients $\{\nabla\hat{P}^{t,i} = \nabla\hat{P}(\Psi^{t,i}); 1\le i\le k\}$. Let $\bar{P}^{t,k}$ denote a linear approximation of $\hat{P}^{t,k}$ close to $\Psi^{t,k}$ at iteration i, $1\le i\le k$, it implies

$$\bar{P}^{t,k} = \underset{1\le i\le k}{Max}\left\{\nabla\hat{P}^{t,i}(\Psi^t - \Psi^{t,i}) + \hat{P}^{t,i}\right\} \tag{28}$$

Let

$$e_{i,k}^t = \hat{P}^{t,k} - (\hat{P}^{t,i} + \nabla\hat{P}^{t,i}(\Psi^{t,k} - \Psi^{t,i})) \tag{29}$$

denote an error bound for a linear approximation of $\hat{P}^{t,k}$. A linear approximation of $\hat{P}^{t,k}$ can be expressed in terms of period-dependent gradients.

$$\bar{P}^{t,k} = \underset{1\le i\le k}{Max}\left\{\nabla\hat{P}^{t,i}(\Psi^t - \Psi^{t,k}) - e_{i,k}^t\right\} + \hat{P}^{t,k} \tag{30}$$

Therefore, a period-dependent cutting plane for (26) can be expressed as follows.

$$\underset{\Psi^t\in\Pi^t}{Min}\bar{P}^{t,k} = \underset{\Psi^t\in\Pi^t}{Min}\underset{1\le i\le k}{Max}\left\{\nabla\hat{P}^{t,i}(\Psi^t - \Psi^{t,k}) - e_{i,k}^t\right\} + \hat{P}^{t,k} \tag{31}$$

In (31), the minimization of $\bar{P}^{t,k}$ corresponds to one step of cutting plane model that may induce slow convergence. To effectively solve (26) with considerable reductions in period-dependent PI, a novel bundle model using a quadratic stabilized term via a predetermined parameter m_k is presented to reliably solve the minimization of $\bar{P}^{t,k}$. For every time period $t,\forall t\in T$, and for given period-dependent signal setting $\Psi^{t,k}$, we have

$$\underset{\Psi^t\in\Pi^t}{Min}\;\bar{P}^{t,k} = z^t + \frac{1}{2}(\Psi^t - \Psi^{t,k})m_k(\Psi^t - \Psi^{t,k})$$
$$subject\ to\ \ \nabla\hat{P}^{t,i}(\Psi^t - \Psi^{t,k}) - e_{i,k}^t + \hat{P}^{t,k} \le z^t, 1\le i\le k \tag{32}$$

4.3. A level set bundle method

A period-dependent bundle set method aiming to attenuating iterative gap between (24) and (25) is presented as follows. Let $\hat{\Psi}^{t,k}$ solve (32) and let $\delta^{t,k}$ denote a gap between (24) and (25) such that

$$\delta^{t,k} = \hat{P}^{t,k} - \breve{P}^{t,k},\ \forall t\in T \tag{33}$$

Introduce a period-dependent level set for (33):

$$\Theta^{t,k} = \left\{\Psi^t\in\Pi^t, \bar{P}^{t,k} \le \breve{P}^{t,k} + l\delta^{t,k}\right\} \tag{34}$$

with $l\in[0,1]$. Let $\Pr_{\Theta^{t,k}}(\hat{\Psi}^{t,k})$ denote the projection of $\hat{\Psi}^{t,k}$ on a level set $\Theta^{t,k}$ such that

$$\left\|\breve{\Psi}^{t,k} - \Pr_{\Theta^{t,k}}(\breve{\Psi}^{t,k})\right\| = \inf_{x\in\Theta^{t,k}}\left\|\breve{\Psi}^{t,k} - x\right\| \tag{35}$$

A tentative solution for (32) can be presented as follows.

$$\breve{\Psi}^{t,k} = \underset{\Theta^{t,k}}{\Pr}(\hat{\Psi}^{t,k}) \tag{36}$$

A sequence of iterates $\{\Psi^{t,k}\}$ can be determined in accordance with

$$\Psi^{t,k+1} = \underset{\Pi^t}{\Pr}(\Psi^{t,k} + \tau(\breve{\Psi}^{t,k} - \Psi^{t,k})), \qquad \forall k = 1,2,... \tag{37}$$

where $\tau\in(0,2)$ is the step length which minimizes $\bar{P}^{t,k}$ in (32).

Theorem 1 (A level set bundle method with projection). Let Ψ^* be a minimum point of (37), then for every period t, $\|\Psi^{t,k} - \Psi^*\|$ is monotonically decreasing, and $\|\Psi^{t,k} - \Psi^*\| \le \|\Psi^{t,1} - \Psi^*\|$, i.e. the sequence of points $\{\Psi^{t,k}\}$, $\forall t\in T$ generated by a level set bundle method with projection is bounded.

Proof. For any x and y, by definition of the projection, we have

$$\|\Pr(x) - \Pr(y)\| \le \|x - y\| \tag{38}$$

thus for $\Psi^{t,k+1}$ we have

$$\begin{aligned}\left\|\Psi^{t,k+1} - \Psi^*\right\|^2 &= \left\|\Pr_{\Pi^t}(\Psi^{t,k} + \tau(\breve{\Psi}^{t,k} - \Psi^{t,k})) - \Psi^*\right\|^2 \\ &\le \left\|\Psi^{t,k} + \tau(\breve{\Psi}^{t,k} - \Psi^{t,k}) - \Psi^*\right\|^2 \\ &= \left\|\Psi^{t,k} - \Psi^*\right\|^2 + \tau^2\left\|(\breve{\Psi}^{t,k} - \Psi^{t,k})\right\|^2 \\ &\quad + 2\tau(\Psi^{t,k} - \Psi^*)(\breve{\Psi}^{t,k} - \Psi^{t,k})\end{aligned} \tag{39}$$

let $\breve{\Psi}^{t,k} = \Psi^*$, thus in (39)

$$\begin{aligned}\left\|\Psi^{t,k+1} - \Psi^*\right\|^2 &\le \left\|\Psi^{t,k} - \Psi^*\right\|^2 + \tau^2\left\|(\Psi^* - \Psi^{t,k})\right\|^2 \\ &\quad - 2\tau(\Psi^{t,k} - \Psi^*)(\Psi^{t,k} - \Psi^*) \\ &= \left\|\Psi^{t,k} - \Psi^*\right\|^2 + \tau(\tau-2)\left\|(\Psi^* - \Psi^{t,k})\right\|^2\end{aligned} \tag{40}$$

Since $\tau\in(0,2)$, we have $\|\Psi^{t,k+1} - \Psi^*\|^2 < \|\Psi^{t,k} - \Psi^*\|^2$ for $k = 1,2,....$ It implies $\|\Psi^{t,k} - \Psi^*\|$ is monotonically decreasing, and $\|\Psi^{t,k} - \Psi^*\| \le \|\Psi^{t,1} - \Psi^*\|, \forall t\in T$. □

4.4. A two-stage solution scheme

A flexible signal control (FLS) can be determined by a following two-stage solution scheme as shown in Fig. 1.

Step 1. For every period t, $\forall t\in T$, start with period-dependent signal control $\Psi^{t,k}$ and scenario-based probability $p^{t,k}$ of uncertain risk in the presence of hazmat transportation. Set iteration index $k = 1$ and a stopping threshold $\varepsilon^{t,k}$.

Step 2. Stage I: solving a maximization (24) for $p^{t,k}$ with signal setting $\Psi^{t,k}$ and obtain an upper bound $\hat{P}^{t,k}$.

Step 3. Stage II: solving a minimization (25) for lower bound $\breve{P}^{t,k}$ with probability $p^{t,k}$ of uncertain link risk via a period-dependent cutting plane (29).

Step 4. Calculate a bound gap by (33). Construct a level set via (34) and find new signal setting $\Psi^{t,k+1}$ via (37).

Step 5. Bound check: if the bound gap $\delta^{t,k}$ is within a threshold $\varepsilon^{t,k}$, then stop and $\Psi^{t,k+1}$ is the solution for MPEC (18). Otherwise, move iteration k to $k+1$ and go to Step 2.

5. Numerical computations and comparisons

To investigate resilience of FLS for multi-period travel demand against uncertain link risk in the presence of hazmat transportation, numerical computations and comparisons with existing signal control are

Table 1
Base period 1 travel demands for Allsop and Charlesworth's road network (in veh/h).

Origin/destination	A	B	D	E	F	Origin totals
A	–	250	700	30	200	1180
C	40	20	200	130	900	1290
D	400	250	–	50	100	800
E	300	130	30	–	20	480
G	550	450	170	60	20	1250
Destination totals	1290	1100	1100	270	1240	5000

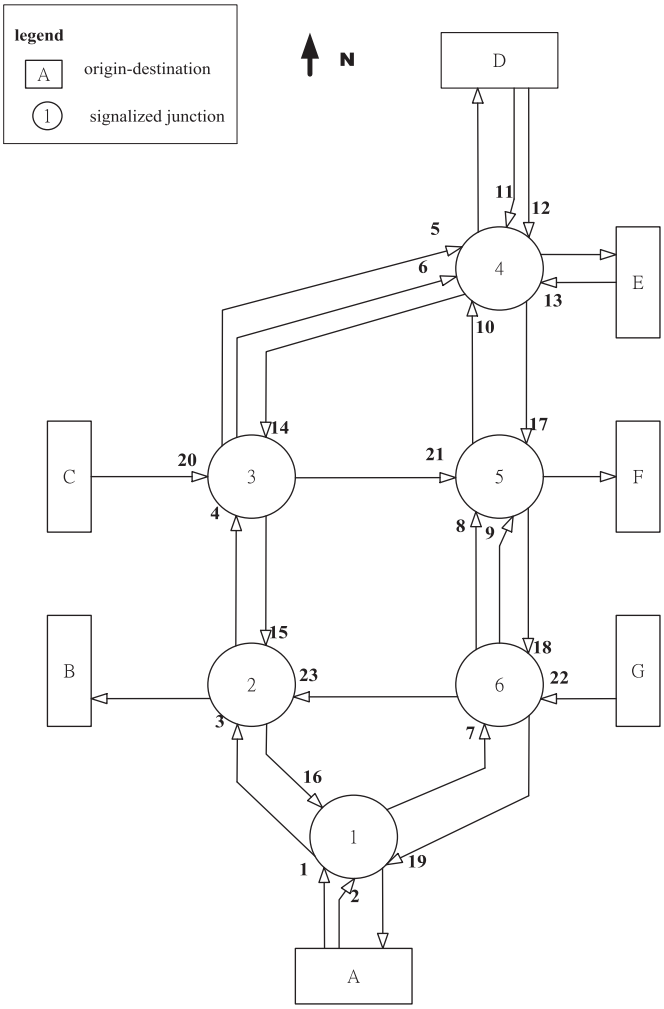

Fig. 2. Layout for Allsop and Charlesworth's network.

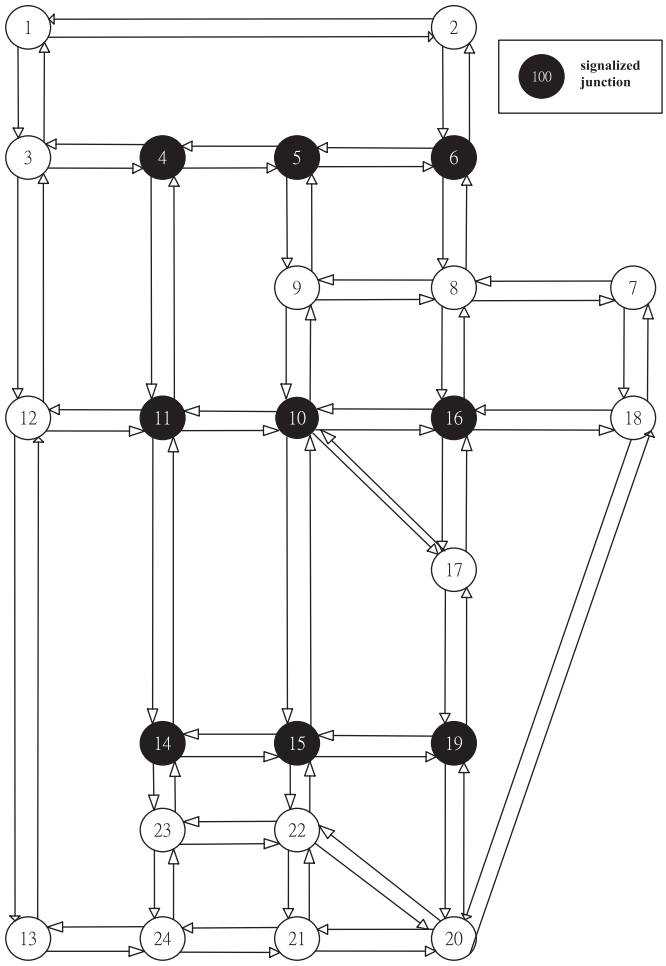

Fig. 3. Sioux Falls network with 9 signalized junctions.

performed using example road network [29,30] as shown in Figs. 2 and 3. As it can be observed in Fig. 2, this example road network includes 22 pairs of OD pair-ends, 23 links and 6 signal-controlled junctions. Two-period initial travel demand for pairs of OD are given in Tables 1 and 2 together with cruise travel times in Table 3. Given average travel speed over periods for regular traffic on links, the average length on a link can be calculated as the product of average speed and cruise travel time along the link. Provided that average population on the link length is known a priori, incidental consequence of accidental release of vehicles carrying dangerous materials can be estimated by a duration-population-frequency risk measure as in [17]. Initial two-period signal control for Allsop and Charlesworth's road network [29] are also given in Table 4. In order to understand the effectiveness of FLS when performed in real world, as shown in Fig. 3, a real data Sioux Falls city network with 9 signal-controlled junctions [30] is considered. Numerical comparisons in single period OD demand with existing robust signal control like SR [24] and ER [20] are made and results are summarized in Figs. 4–9. For multi-period OD demand, comparisons are also made with MSR [21] and MSP [23], and numerical results are summarized in Figs. 10–15. In the following computations, the minimum green time for each signal-controlled group is 7 s using typical values found in practice, and the clearance times are 5 s between incompatible signal groups. The maximum cycle time is set at 180 s. The stopping criterion used in solution scheme is set when the relative gap in (33) is less than 0.15%. Implementations for carrying out computations are made on DELL T7610, Intel Xeon 2.5 GHz processor with 32 GB RAM under Windows 10 using C++ compiler.

Table 2
Base period 2 travel demands for Allsop and Charlesworth's road network (in veh/h).

Origin/destination	A	B	D	E	F	Origin totals
A	–	250	700	30	200	1180
C	140	120	200	130	900	1490
D	400	250	–	200	100	950
E	300	130	180	–	20	630
G	550	450	170	60	20	1250
Destination totals	1390	1200	1250	420	1240	5500

Table 3
Cruise travel time for Allsop and Charlesworth's road network.

Junction no.	Link no.	Cruise travel time (in sec)	Junction no.	Link no.	Cruise travel time (in sec)
1	1	0	4	10	10
1	2	0	4	11	0
1	16	10	4	12	0
1	19	10	4	13	0
2	3	10	5	8	15
2	15	15	5	9	15
2	23	15	5	17	10
3	4	15	5	21	15
3	14	20	6	7	10
3	20	0	6	18	15
4	5	20	6	22	0
4	6	20			

Table 4
Initial data set for 2-period Allsop & Charlesworth' s road network.

Signal control	Period 1	Period 2
$1/\zeta^t$	70	75
ϕ^t_{11}/ζ^t	30	32
ϕ^t_{21}/ζ^t	30	33
ϕ^t_{31}/ζ^t	70	75
ϕ^t_{12}/ζ^t	30	32
ϕ^t_{22}/ζ^t	30	33
ϕ^t_{13}/ζ^t	30	32
ϕ^t_{23}/ζ^t	30	33
ϕ^t_{14}/ζ^t	18	20
ϕ^t_{24}/ζ^t	18	20
ϕ^t_{34}/ζ^t	19	20
ϕ^t_{44}/ζ^t	41	45
ϕ^t_{54}/ζ^t	42	45
ϕ^t_{15}/ζ^t	18	20
ϕ^t_{25}/ζ^t	18	20
ϕ^t_{35}/ζ^t	19	20
ϕ^t_{45}/ζ^t	41	45
ϕ^t_{16}/ζ^t	30	32
ϕ^t_{26}/ζ^t	30	33
PI (in $)	5.17e5	7.87e5

where for every period t, $1/\zeta^t$denotes the common cycle time and ϕ^t_{jm}/ζ^t denotes the green durations in seconds for signal group j at junction m.

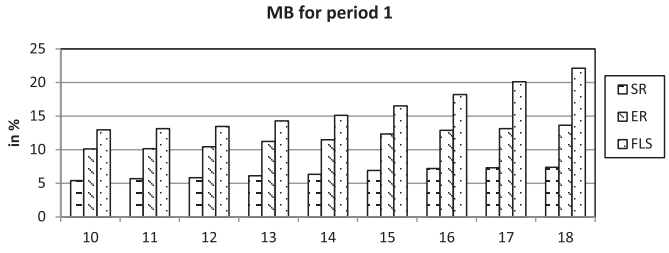

Fig. 4. MB for resilient signal control with uncertain risk.

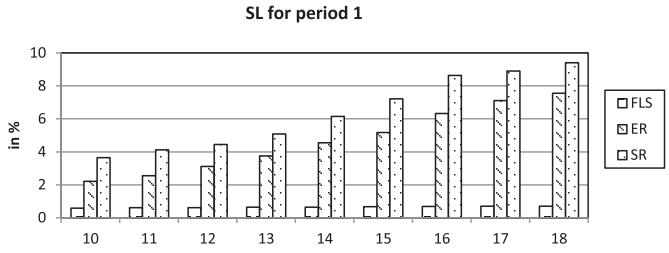

Fig. 5. SL for resilient signal control with uncertain risk.

5.1. Computational results

According to proposed two-stage solution scheme as shown in Fig. 1, numerical results for FLS with two-period data set are summarized in Tables 5–8 with varying weights for PI in (16) and various levels of link risk uncertainty budget $\Gamma, \Gamma = \{0, 5, 7, 10\}$. As it can be seen in Tables 5 and 6, the PI values rapidly grows as more weights being considered on probablistic duration-population-frequency risk measure for two-period OD demand, and PI values apparently become stable as weighting parameter is over 0.5. As it can be seen in Tables 7 and 8, FLS under various level of budget makes considerable reductions in PI by 32% and 55% respectively for two-period OD demand. In accordance with solution scheme in Fig. 1, numerical results for FLS over iterations, taking $\Gamma = 10$ with weighting parameter $\alpha = .5$ for example, can be detailed in Tables 9 and 10. As it is shown in Table 9 for period 1, the relative gap in column 4 between upper bound in column 2 and lower bound in column 3 is reduced iteratively as computation proceeds. According to Fig. 1, the gradients in column 5 in Table 9 for Stage II are iteratively increased. The gradients in column 6 in Table 9 for Stage I are also iteratively decreased. It takes 16 iterations to obtain optimal signal control. For period 2, similarly, as it can be seen in Table 10, the relative gap in column 4 between upper and lower bounds can be reduced from

Table 5
Resilient signal control for period 1 with $\Gamma = 10$.

Period-dependent signal control	$\alpha = .01$	$\alpha = .1$	$\alpha = .5$	$\alpha = .9$	$\alpha = .99$
$1/\zeta^t$	106	105	120	118	125
ϕ^t_{11}/ζ^t	35	47	54	50	57
ϕ^t_{21}/ζ^t	61	48	56	58	58
ϕ^t_{31}/ζ^t	106	105	120	118	125
ϕ^t_{12}/ζ^t	65	49	56	54	59
ϕ^t_{22}/ζ^t	31	46	54	54	56
ϕ^t_{13}/ζ^t	39	47	55	55	55
ϕ^t_{23}/ζ^t	57	48	55	53	60
ϕ^t_{14}/ζ^t	34	30	35	33	35
ϕ^t_{24}/ζ^t	27	30	35	34	35
ϕ^t_{34}/ζ^t	30	30	35	36	40
ϕ^t_{44}/ζ^t	66	65	75	72	75
ϕ^t_{54}/ζ^t	69	65	75	74	80
ϕ^t_{15}/ζ^t	19	38	35	36	43
ϕ^t_{25}/ζ^t	29	24	35	34	24
ϕ^t_{35}/ζ^t	43	28	35	33	43
ϕ^t_{45}/ζ^t	53	67	75	65	72
ϕ^t_{16}/ζ^t	50	46	51	54	56
ϕ^t_{26}/ζ^t	46	49	59	54	59
PI (in $)	3.36e5	3.37e5	3.55e5	3.55e5	3.56e5
CPU (in sec)	176	188	178	178	192

Table 6
Resilient signal control for period 2 with $\Gamma = 10$.

Period-dependent signal control	$\alpha = .01$	$\alpha = .1$	$\alpha = .5$	$\alpha = .9$	$\alpha = .99$
$1/\zeta^t$	130	118	130	120	125
ϕ^t_{11}/ζ^t	58	54	60	55	57
ϕ^t_{21}/ζ^t	62	54	60	55	58
ϕ^t_{31}/ζ^t	130	118	130	120	125
ϕ^t_{12}/ζ^t	60	54	60	54	60
ϕ^t_{22}/ζ^t	60	54	60	56	55
ϕ^t_{13}/ζ^t	60	54	60	55	55
ϕ^t_{23}/ζ^t	60	54	60	55	60
ϕ^t_{14}/ζ^t	37	35	37	35	35
ϕ^t_{24}/ζ^t	39	35	39	35	35
ϕ^t_{34}/ζ^t	39	33	39	35	40
ϕ^t_{44}/ζ^t	81	75	81	75	75
ϕ^t_{54}/ζ^t	81	73	81	75	80
ϕ^t_{15}/ζ^t	38	35	38	35	43
ϕ^t_{25}/ζ^t	37	35	37	35	24
ϕ^t_{35}/ζ^t	40	33	40	35	43
ϕ^t_{45}/ζ^t	80	75	80	75	72
ϕ^t_{16}/ζ^t	61	54	60	58	55
ϕ^t_{26}/ζ^t	59	54	60	52	60
PI (in $)	3.37e5	3.37e5	3.55e5	3.55e5	3.56e5
CPU (in sec)	185	190	178	187	185

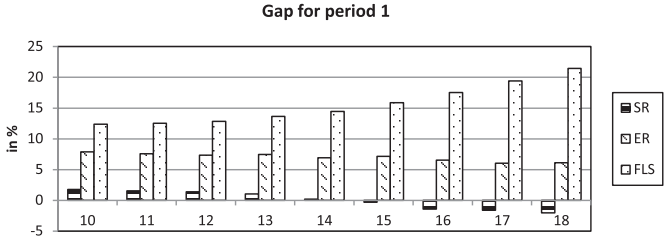

Fig. 6. Gap for resilient signal control with uncertain risk.

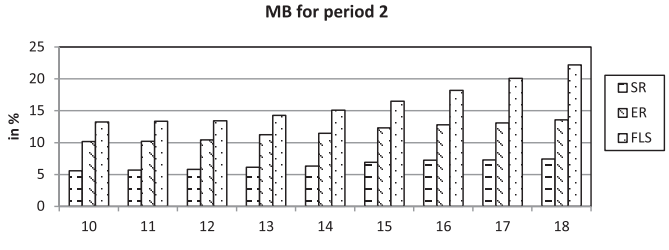

Fig. 7. MB for resilient signal control with uncertain risk.

iteration to iteration. According to Fig. 1, the corresponding gradients in column 5 for Stage II minimization are increased iteratively as shown in Table 10. The gradients in column 6 for Stage I maximization are also decreased from iteration to iteration as shown in Table 10. It takes 14 iterations to obtain optimal signal control.

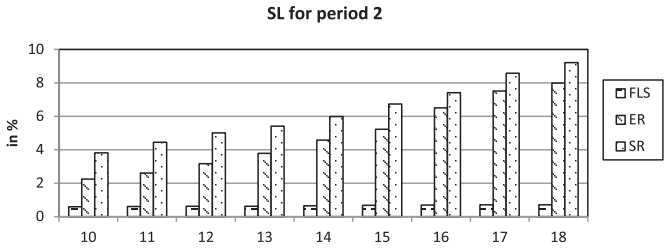

Fig. 8. SL for resilient signal control with uncertain risk.

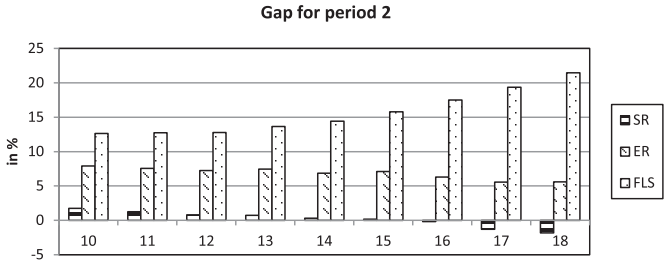

Fig. 9. Gap for resilient signal control with uncertain risk.

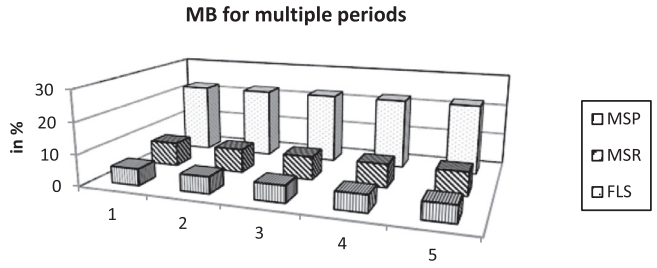

Fig. 10. MB for resilient signal control over multi-period.

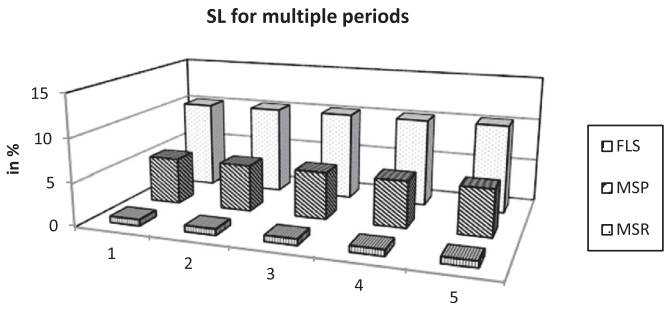

Fig. 11. SL for resilient signal control over multi-period.

5.2. Computational comparisons with other signal controls

In order to quantify resilience of linked signal control FLS against worst-case scenarios of uncertain risk under hazmat carriers in multiple periods of OD demands, the model benefit for resilient linked signal (MB) can be introduced first. For every period $t, \forall t \in T$, let P_R^t and Z_R^t denote robust and nominal solutions against high consequence of link risk. A period-dependent percent benefit ratio of model given by resilient signal control against high consequence of link risk over those did the nominal one can be described as follows.

$$\sigma_R^t = 100 * \left(\frac{Z_R^t - P_R^t}{P_R^t} \right)\% \tag{41}$$

On the other hand, in order to balance trade-off of resilient linked signal controls in nominal situation, a solution loss (SL) in optimality under deterministic situations can be introduced as follows. For every

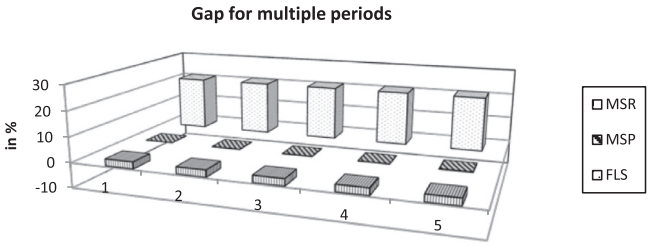

Fig. 12. Gap for resilient signal control over multi-period.

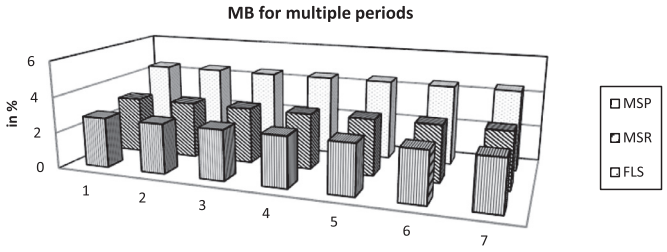

Fig. 13. MB for resilient signal control at Sioux Falls network.

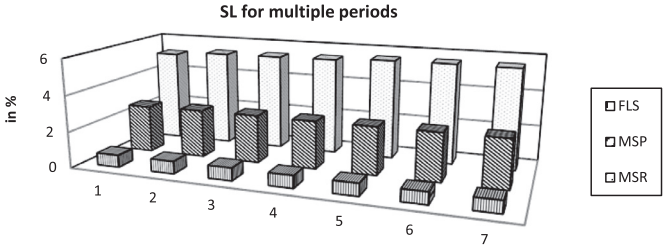

Fig. 14. SL for resilient signal control at Sioux Falls network.

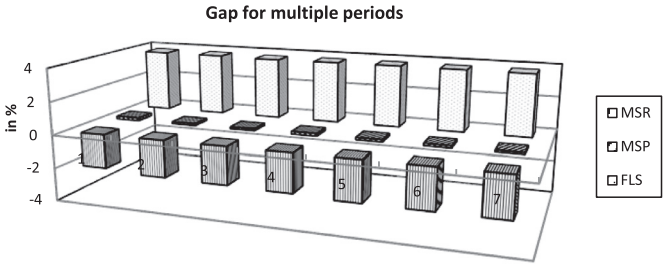

Fig. 15. Gap for resilient signal control at Sioux Falls network.

period $t, \forall t \in T$, let P_D^t and Z_D^t denote robust and nominal solutions in deterministic situations. A period-dependent percent loss ratio of solutions (SL) given by resilient linked signal control over those did in nominal situation can be described.

$$\sigma_D^t = 100 * \left(\frac{P_D^t - Z_D^t}{Z_D^t} \right)\% \tag{42}$$

Computational results for FLS in 2-period with various levels of uncertain link risk can be found in Tables 11 and 12. As it can be seen in Table 11, the resilience of FLS quantified by MB in (41) can be of as high as 12.97% when level of uncertainty budget is 10 while the solution loss quantified by SL in (42) being of as low as nearly 0.6%. Similarly, as shown in Table 12, the resilience of FLS in MB can be of as high as 13.25% while the solution loss in SL being of as low as nearly 0.6%.

In order to understand resilience of existing signal control such as SR [24], ER [20], MSR [21], and MSP [23] under hazmat carriers in multiple periods, computations and comparisons in two-period and multi-period of OD demands are made, and numerical results are respectively

Table 7
Resilient signal control for period 1 with $\alpha = .5$.

Period-dependent signal control	$\Gamma = 0$	$\Gamma = 5$	$\Gamma = 7$	$\Gamma = 10$
$1/\zeta^t$	106	105	118	120
ϕ^t_{11}/ζ^t	35	47	49	54
ϕ^t_{21}/ζ^t	61	48	59	56
ϕ^t_{31}/ζ^t	106	105	118	120
ϕ^t_{12}/ζ^t	66	49	55	56
ϕ^t_{22}/ζ^t	30	46	53	54
ϕ^t_{13}/ζ^t	39	47	55	55
ϕ^t_{23}/ζ^t	57	48	53	55
ϕ^t_{14}/ζ^t	34	30	33	35
ϕ^t_{24}/ζ^t	27	30	34	35
ϕ^t_{34}/ζ^t	30	30	36	35
ϕ^t_{44}/ζ^t	66	65	72	75
ϕ^t_{54}/ζ^t	69	65	74	75
ϕ^t_{15}/ζ^t	19	38	36	35
ϕ^t_{25}/ζ^t	29	24	34	35
ϕ^t_{35}/ζ^t	43	28	33	35
ϕ^t_{45}/ζ^t	53	67	65	75
ϕ^t_{16}/ζ^t	49	46	55	51
ϕ^t_{26}/ζ^t	47	49	53	59
PI (in $)	3.46e5	3.49e5	3.51e5	3.55e5
CPU (in sec)	176	182	180	178

Table 8
Resilient signal control for period 2 with $\alpha = .5$.

Period-dependent signal control	$\Gamma = 0$	$\Gamma = 5$	$\Gamma = 7$	$\Gamma = 10$
$1/\zeta^t$	130	118	120	130
ϕ^t_{11}/ζ^t	58	54	56	60
ϕ^t_{21}/ζ^t	62	54	54	60
ϕ^t_{31}/ζ^t	130	118	120	130
ϕ^t_{12}/ζ^t	60	54	55	60
ϕ^t_{22}/ζ^t	60	54	55	60
ϕ^t_{13}/ζ^t	60	54	55	60
ϕ^t_{23}/ζ^t	60	54	55	60
ϕ^t_{14}/ζ^t	37	35	35	37
ϕ^t_{24}/ζ^t	39	35	35	39
ϕ^t_{34}/ζ^t	39	33	35	39
ϕ^t_{44}/ζ^t	81	75	75	81
ϕ^t_{54}/ζ^t	81	73	75	81
ϕ^t_{15}/ζ^t	38	35	35	38
ϕ^t_{25}/ζ^t	37	35	35	37
ϕ^t_{35}/ζ^t	40	33	35	40
ϕ^t_{45}/ζ^t	80	75	75	80
ϕ^t_{16}/ζ^t	61	54	56	60
ϕ^t_{26}/ζ^t	59	54	54	60
PI (in $)	3.47e5	3.50e5	3.53e5	3.55e5
CPU (in sec)	181	182	181	178

summarized in Figs. 4–9 and Figs. 10–12. First, consider a two-period OD demand with fixed weight $\alpha = .5$ and a variety of uncertain link risk budget Γ, $\Gamma \in [10, 18]$. Comparisons for resilience of linked signal control in 2-period quantified by MB and SL can be numerically made and summarized in Figs. 4–6 and Figs. 7–9 respectively. As it can be seen in Figs. 4 and 7, FLS exhibits a relatively high resilience in MB than those did ER followed by SR in a single-period of travel demand. As it can be observed in Figs. 5 and 8, on the other hand, SR and ER incur relatively high optimality loss in SL for both periods. As it has been widely noticed in literature, SR can incur great optimality loss in deterministic conditions due to a norm-bounded design of traffic link risk in a predetermined likelihood region of uncertainty. As it can be seen in Fig. 5, as expected, SR for period 1 can incur a very high SL of 6% when level of link risk uncertainty budget is more than 14. ER incurs a moderately high SL of 7.56% when level of link risk uncertainty budget achieves 18.

Table 9
Resilient signal control for period 1 with $\alpha = .5$when $\Gamma = 10$.

$\Psi^{1,k}$	$\hat{P}^{1,k}$ (in $)	$\check{P}^{1,k}$ (in $)	$\frac{\hat{\delta}^{1,k}}{\hat{P}^{1,k}} * 100\%$	$\nabla\hat{P}^{1,k}$	$\nabla\check{P}^{1,k}$
$\Psi^{1,1}$	517,000	127,800	75.28	−2316.5	2122.5
$\Psi^{1,2}$	499,800	131,500	73.69	−1785.6	1851.6
$\Psi^{1,3}$	487,500	155,600	68.08	−1113.6	1452.3
$\Psi^{1,4}$	479,600	175,000	63.51	−975.6	965.4
$\Psi^{1,5}$	467,500	205,000	56.15	−715.1	725.6
$\Psi^{1,6}$	458,500	227,000	50.49	−485.0	525.4
$\Psi^{1,7}$	441,000	285,000	35.37	−353.1	324.9
$\Psi^{1,8}$	425,500	295,100	30.65	−265.1	260.7
$\Psi^{1,9}$	411,500	305,000	25.88	−185.9	185.8
$\Psi^{1,10}$	398,500	312,000	21.71	−125.3	139.1
$\Psi^{1,11}$	388,500	328,500	15.44	−85.5	86.8
$\Psi^{1,12}$	380,500	335,500	11.83	−68.2	63.4
$\Psi^{1,13}$	372,500	340,500	8.59	−32.5	35.1
$\Psi^{1,14}$	368,500	341,500	7.33	−12.8	12.5
$\Psi^{1,15}$	359,500	355,100	1.22	−5.2	5.1
$\Psi^{1,16}$	355,000	355,000	0.00	−0.7	0.5

Table 10
Resilient signal control for period 2 with $\alpha = .5$when $\Gamma = 10$.

$\Psi^{2,k}$	$\hat{P}^{2,k}$ (in $)	$\check{P}^{2,k}$ (in $)	$\frac{\hat{\delta}^{2,k}}{\hat{P}^{2,k}} * 100\%$	$\nabla\hat{P}^{2,k}$	$\nabla\check{P}^{2,k}$
$\Psi^{2,1}$	787,000	125,000	84.12	−3130.44	2786.5
$\Psi^{2,2}$	761,500	131,500	82.73	−2154.12	1955.3
$\Psi^{2,3}$	695,000	151,000	78.27	−1650.65	1567.5
$\Psi^{2,4}$	675,000	172,000	74.52	−932.76	911.2
$\Psi^{2,5}$	655,000	201,000	69.31	−651.77	671.2
$\Psi^{2,6}$	587,500	225,000	61.70	−423.55	435.6
$\Psi^{2,7}$	505,000	274,000	45.74	−274.66	251.9
$\Psi^{2,8}$	455,000	298,000	34.51	−125.44	112.8
$\Psi^{2,9}$	412,000	312,000	24.27	−52.98	45.5
$\Psi^{2,10}$	385,000	325,000	15.58	−21.17	22.8
$\Psi^{2,11}$	367,000	335,000	8.72	−14.86	12.9
$\Psi^{2,12}$	363,000	345,000	4.96	−7.56	6.5
$\Psi^{2,13}$	361,000	348,000	3.60	−2.15	1.86
$\Psi^{2,14}$	355,000	355,000	0.00	−0.66	0.5

Table 11
Resilient signal control for period 1 with $\alpha = .5$.

Γ	Z^t_D(in $)	P^t_R(in $)	P^t_D (in $)	Z^t_R(in $)	σ^t_R (%)	σ^t_D (%)
0	346,000	346,000	346,000	346,000	–	–
5	346,000	349,000	346,800	365,050	4.60	0.23
7	346,000	351,000	347,200	378,580	7.86	0.35
10	346,000	355,000	348,050	401,040	12.97	0.59

Table 12
Resilient signal control for period 2 with $\alpha = .5$.

Γ	Z^t_D(in $)	P^t_R(in $)	P^t_D (in $)	Z^t_R(in $)	σ^t_R (%)	σ^t_D (%)
0	347,000	347,000	347,000	347,000	–	–
5	347,000	350,000	347,450	366,400	4.69	0.13
7	347,000	353,000	348,350	379,950	7.63	0.39
10	347,000	355,000	349,050	402,050	13.25	0.59

For period 2, as it is shown in Fig. 8, similarly, SR can incur a very high SL of 7% when level of link risk uncertainty budget is more than 16. ER again incurs a moderately high SL of nearly 8% when level of link risk uncertainty budget achieves 18. By contrast, FLS exhibits a good attenuation in SL of nearly 0.7% when level of link risk uncertainty budget achieves 18. The relative gaps between MB and SL can be also found

in Figs. 6 and 9 for FLS, ER, and SR. For period 1, FLS achieves a relatively high gap of nearly 21% when level of link risk uncertainty budget achieves 18 followed by ER. As it has been noticed in [20], ER can incur an increasing high optimality loss in SL as level of uncertainty grows in single periods. As expected, the relative gap between MB and SL for ER become gradually decreased when level of link risk uncertainty budget increases from 13 to 18 as demonstrated in Fig. 6. For period 2, FLS, again, exhibits a moderately high gap of nearly 21% followed by ER. The relative gaps of ER between MB and SL, again, become gradually decreased as level of link risk uncertainty budget increases from 16 to 18 as shown in Fig. 9.

Secondly, consider multiple periods of OD travel demand with uncertain link risk $\Gamma = 20$. Numerical results and comparisons can be performed and plotted in Figs. 10–12 for MSR and MSP. As it can be seen in Fig. 10, FLS achieves a relatively high MB than those did MSP followed by MSR over a successive 5-period of travel demand. On the other hand, as shown in Fig. 11, MSR and MSP incur a relatively high optimality loss quantified by SL than those did FLS. Moreover, MSP using a sample average approximation for link risk uncertainty incurs a moderately less SL of nearly 5.4% as compared to those of nearly 10% did MSR over all 5-period of OD demands. The relative gap for FLS, MSR, and MSP can be computed and summarized in Fig. 12. As it can be seen in Fig. 12, FLS achieves a most high gap of nearly 22%. As expected, a set-based MSR can incur a rather high optimality loss in SL, and it leads to a least negative gap of nearly 3% between MB and SL.

5.3. Applications to a real-data Sioux Falls city road network

To investigate the feasibility and effectiveness of FLS on a real-data road network in multi-period of OD travel demand, in this section, numerical computations and comparisons with MSP and MSR using Sioux Falls city road network are made. Numerical results are summarized in Figs. 13–15 for a successive 7-period of OD travel demand. As it can be seen in Fig. 13, again, FLS achieves a most high resilience in MB of nearly 4.5% in all cases followed by MSR of nearly 3% while MSP achieving a least resilience of nearly below 3% in all cases. As also shown in Fig. 14, FLS can incur a least optimality loss in SL of nearly 0.8% followed by MSP of moderately high 2.7%. The relative gap between MB and SL, as shown in Fig. 15, for FLS can be as high as of nearly 4%. However, the relative gaps between MB and SL for MSP and MSR continue to attenuate over protracted periods. As it can be seen in Fig. 15, the relative gap for MSP can be of marginal value over a 7-period of travel demand. Moreover, the relative gap for MSR under hazmat carriers can be of negative 3% due to growing uncertain risk over successive protracted periods.

6. Conclusions and discussions

In this paper, a traffic-responsive linked signal control for multi-period OD demands has been proposed to quantify resilience of road network under hazmat carriers. To effectively quantify resilience of period-dependent linked traffic signals, a simple performance index for linked signals is presented through a pre-determined parameter between period-dependent traffic queues and period-dependent risk measure. Period-dependent adaptability for linked signal control can be effectively sustained from the taking of traffic-responsive signal controls, and also from period-dependent path choices that are responsive to proactive signal settings. Period-dependent travel delay and risk over entire road network can be effectively estimated through interdependent travel cost between regular traffic and hazmat carriers when users' equilibrium can be achieved efficiently between regular road users and hazmat carriers. The interdependency of period-dependent linked signals can be regarded as part CI in area wide road traffic networks. The resilience of CI can be estimated by linear combination of period-dependent traffic queues at downstream signalized junctions and duration-population-frequency risk measure in the presence of hazmat carriers. In this paper, period-dependent interdependency arising from the need for estimating period-dependent traffic delay incurred at downstream linked signals between regular traffic users and hazmat carriers has been fully taken into account. In contrast to earlier work in [8,10] where inherent uncertainties are considered as a priori, we proposed a two-stage min-max model instead to quantify traffic-responsive and resilient linked signal control in multiple periods under uncertain risk due to hazmat carriers. Accordingly, a two-stage robust model has also been proposed to highlight the resilience of linked signal control of area wide traffic road network in worst-case scenarios. A mathematical program with equilibrium constraints (MPEC) has been first proposed while considering path choices between regular road users and hazmat carriers in multi-period OD travel demands. Numerical computations and comparisons using real-data road network have been made with existing signal controls for multi-period OD travel demands. These results reported obviously indicate that proposed flexible signal control can be more resilient than existing ones against a high-consequence of exposure risk in the presence of hazmat transportation.

For urban city road network with coordinated signal control, severe time-dependent traffic congestion can give rise to direct or indirect impact on vulnerability of road networks for all road users. Consider some signal-controlled junctions as part of critical infrastructure components in urban city road networks, which can have interdependency with the ones at upstream and others at downstream through time-varying traffic flows. In order to effectively quantify vulnerable links of road network for time-varying OD travel demands using time-dependent signal control that can enhance overall resilience of transportation infrastructure, as it has been currently received growing attention [1,8,31]. The proposed FLS in this paper has taken a first step toward achieving this purpose. In the near future, we continue to work in this regard which can be stated in the following points.

(1) In order to understand interdependency between critical signal-controlled junctions and connected links in city road networks, more elaborate modelling for time-dependent traffic flow is being underway. This paper sheds some light on proposing period-dependent linked signal control using a mathematical program while considering road users' route choice. For time-dependent travel demand and traffic flow distribution, the model presented in this paper can be extended and used to effectively quantify time-dependent vulnerable links of signalized junctions in urban road networks with resulting consequence for road users concerned by vulnerable links under uncertainty.
(2) In order to characterize vulnerable links with high opportunity in capacity loss due to time-dependent congestion that can potentially give rise to cascading overflow at downstream junctions, a time-dependent metric accounting for redundant capacity on each link needs to be considered. This paper used a simple bi-objective minimization between period-dependent queue and traffic risk on average through a pre-determined parameter without accounting for identification of fragility of vulnerable link capacity due to potential cascading time-varying congestion. For time-varying travel demand and traffic flow, the model presented in this paper can be extended to account for time-dependent traffic delay and characterize vulnerability of traffic road networks quantitatively under uncertainty when a multi-objective performance metric is considered to evaluate fragility of signal-controlled links.
(3) Moreover, in order to effectively mitigate vulnerability of general traffic road networks with signalized junctions, it becomes increasingly essential not only to locate important CI of time-dependent signalized links but also to increase overall redundant capacity of entire area wide road networks through advanced signal control [32,33]. In this paper, the proposed FLS is developed only by delay-minimizing performance measure, and none of redundant capacity of signal-controlled link is discussed. As a consequence, computational efficiency of proposed FLS can be undermined at saturated signal-controlled junctions due to lack of consideration of redundant

capacity in signalized links. This paper presented a mathematical program with equilibrium constraints accounting for road users' path choice. The proposed model can be extended to a time-dependent signal control system with saturated links in which redundant capacities of system can be investigated. A time-dependent resilience of system can be furthermore quantified. The time-dependent vulnerable link with high opportunity in capacity loss due to saturated congestion can be effectively identified and mitigated. A time-dependent signal control can be developed on the basis of maximum reserve capacity of time-dependent OD travel demands. For large-sized general road networks with hundreds of decisions and instances, polynomial-type computationally efficient algorithms need to be considered from the perspective of computational complexity. Numerical comparisons using a variety of large-sized road networks with more time-dependent OD pairs can be furthermore considered for these issues of interest, and we will discuss these points in subsequent papers.

Acknowledgements

The author would like to express her gratitude to anonymous reviewers and Editor in Chief for their constructive comments on earlier versions of the manuscript. Many thanks also go to Taiwan National Science Council for financial support via grant MOST 104-2221-E-259-029-MY3.

Appendix A.1. Sensitivity analysis for traffic flow

Consider the feasible set with respect to perturbation in period-dependent signal setting Ψ'^t for period-dependent traffic flow in (3). For every time period t, $\forall t \in T$, introduce

$$\Phi'^t = \{ f'^t : f'^t = \lambda h'^t, \Lambda h'^t = 0, \exists h'^t \in K^t \} \tag{a.1}$$

with

$$K^t = \left\{ h'^t : \begin{array}{l} (i) h_k'^t \quad free, \quad if \quad h_k^{t*} > 0 \\ (ii) h_k'^t \geq 0, \quad if \quad h_k^{t*} = 0, C_k^t = \pi_i^t \\ (iii) h_k'^t = 0, \quad if \quad h_k^{t*} = 0, C_k^t > \pi_i^t \end{array} , \quad \forall k \in R_i, \forall i \in W \right\} \tag{a.2}$$

Also for period-dependent hazmat carriers in (9) and for every time period $t, \forall t \in T$. Introduce

$$\tilde{\Phi}'^t = \{ x'^t : x'^t = \lambda h'^t, \Lambda h'^t = 0, \exists h'^t \in \tilde{K}^t \} \tag{a.3}$$

with

$$\tilde{K}^t = \left\{ h'^t : \begin{array}{l} (i) h_k'^t \quad free, \quad if \quad h_k^{t*} > 0, \\ (ii) h_k'^t \geq 0, \quad if \quad h_k^{t*} = 0, C_k^t = \pi_i^t \\ (iii) h_k'^t = 0, \quad if \quad h_k^{t*} = 0, C_k^t > \pi_i^t \end{array} , \quad \forall k \in R_i, \forall i \in W^H \right\} \tag{a.4}$$

For every period-dependent flow perturbation in sets a.3) and (a.4), the first-order sensitivity analysis of period-dependent traffic flow $\begin{pmatrix} f'^t \\ x'^t \end{pmatrix}$ in (a.3) and (a.4) along perturbation direction Ψ'^t can be determined in the following way. According to ((17), for every $\begin{pmatrix} \tilde{f} \in \Phi'^t \\ \tilde{x} \in \Phi'^t \end{pmatrix}$, it is to find $\begin{pmatrix} f'^t \in \Phi'^t \\ x'^{s,t} \in \tilde{\Phi}'^t, \forall s \end{pmatrix}$ such that

$$\begin{pmatrix} (\nabla_{\Psi'^t} c^t(\Psi^{t*}, f^t)\Psi'^t + \nabla_{f^t} c^t(\Psi^{t*}, f^t) f'^t)(\tilde{f} - f'^t) \geq 0 \\ (\nabla_{\Psi'^t} \tilde{c}^{s,t}(\Psi^{t*}, f^t)\Psi'^t)(\tilde{x} - x'^{s,t}) \geq 0, \forall s \end{pmatrix}, \forall t \in T \tag{a.5}$$

In a.5), the period-dependent gradients $\nabla_{\Psi'^t} c^t(\Psi^{t*}, f^t)$ and $\nabla_{f^t} c^t(\Psi^{t*}, f^t)$ can be evaluated at Ψ^{t*} when perturbations Ψ'^t are specified. For every scenario s, $\nabla_{\Psi'^t} \tilde{c}^{s,t}(\Psi^{t*}, f^t)$ in (a.5), according to ((10), it shows $\nabla_{\Psi'^t} \tilde{c}^{s,t}(\Psi^{t*}, f^t) = \nabla_{\Psi'^t} c^t(\Psi^{t*}, f^t)$. According to Rademacher's theorem [34] for every period t, the sensitivity analysis of period-dependent traffic flow $\begin{pmatrix} f'^t \\ x'^{s,t}, \forall s \end{pmatrix}$ in (a.5) with respect to Ψ'^t can be determined.

Proposition A.1. (Sensitivity analysis for period-dependent traffic flow) Let Σ be any set of zero measure, and let $\Sigma_{(f^t, x^{s,t}, \forall s)}$ be the set of points at which responding flow $\begin{pmatrix} f^t \\ x^{s,t}, \forall s \end{pmatrix}$ fails to be differentiable. For every $\Psi^{t,k} \notin \Sigma$ and $\Psi^{t,k} \notin \Sigma_{(f^t, x^{s,t}, \forall s)}$, let co denote a convex hull, it implies

$$\partial \Omega^t(\Psi^t) = co\left\{ \lim_{k \to \infty} f'^t(\Psi^{t,k}) : \Psi^{t,k} \to \Psi^{t*}, f'^t(\Psi^{t,k}) exist \right\}, \forall t \in T \tag{a.6}$$

and

$$\partial \tilde{\Omega}^t(\Psi^t) = co\left\{ \lim_{k \to \infty} x'^{s,t}(\Psi^{t,k}) : \Psi^{t,k} \to \Psi^{t*}, x'^{s,t}(\Psi^{t,k}) exist, \forall s \in L \right\}, \forall t \in T \tag{a.7}$$

□

A.2. Sensitivity analysis for period-dependent PI

Following results in Section A.1, the first-order sensitivity analysis of a period-dependent PI in (17) can be derived. According to results in (a.6) and (a.7), a simplified MPEC with α, $\alpha \in [0, 1]$ can be expressed. For every time period t, $\forall t \in T$, let

$$\begin{aligned} P_1^t = (1-\alpha) \sum_{a \in L} \left(D_a^t(\Psi^t, f_a^t) W_D M_D + S_a^t(\Psi^t, f_a^t) W_S M_S \right) \\ + \alpha \sum_{a,s \in L} c_a^t r_a^{s,t} x_a^{s,t} p_a^{s,t} M_r, \forall t \in T \end{aligned} \tag{a.8}$$

Sensitivity analysis for period-dependent PI in (a.8) can be expressed as follows.

Proposition A.2. (Sensitivity analysis for period-dependent PI) Let Σ be any set of zero measure, and let $\Sigma_{P_1^t}$ be the set of points at which the objective function P_1^t fails to be differentiable. For every $\Psi^{t,k} \notin \Sigma$ and $\Psi^{t,k} \notin \Sigma_{P_1^t}$, the first order sensitivity analysis of period-dependent PI, $P_1^t(\Psi^t)$ in (a.8) can be characterized as a convex hull of all points of the form $\lim_{k \to \infty} \nabla_{\Psi'^t} P_1^t(\Psi^{t,k})$ where the subsequence $\{\Psi^{t,k}\}$ converges to a limit value Ψ^{t*}, i.e.

$$\begin{aligned} \partial P_1^t(\Psi^{t*}) &= \partial_{\Psi'^t} P_1^t(\Psi^{t*}) \\ &= co\left\{ \lim_{k \to \infty} \nabla_{\Psi'^t} P_1^t(\Psi^{t,k}) : \Psi^{t,k} \to \Psi^{t*}, \nabla_{\Psi'^t} P_1^t(\Psi^{t,k}) exists \right\}, \\ &\quad \forall t \in T \end{aligned} \tag{a.9}$$

□

According to (a.9), the first-order sensitivity analysis for period-dependent PI with α, $\alpha \in [0, 1]$ can be expressed.

$$\begin{aligned} \nabla_{\Psi'^t} P_1^t(\Psi^{t,k}) = (1-\alpha) \sum_{a \in L} \Big(&(\nabla_{\Psi'^t} D_a^t + \nabla_{f^t} D_a^t f'^t) W_D M_D \\ &+ (\nabla_{\Psi'^t} S_a^t + \nabla_{f^t} S_a^t f'^t) W_S M_S \Big) \\ &+ \alpha \sum_{a,s \in L} ((\nabla_{\Psi'^t} c_a^t \Psi'^t + \nabla_{f_a^t} c_a^t f_a'^t) x_a^{s,t} + c_a^t x_a'^{s,t}) r_a^{s,t} p_a^{s,t} M_r, \\ &\forall t \in T \end{aligned} \tag{a.10}$$

References

[1] SW Chiou. Vulnerability analysis of a signal-controlled road network for equilibrium flow. In: FPG Márquez, B Lev (Eds.) Advanced business analytics, Springer International Publishing Switzerland, pp. 109–142.
[2] Bell MGH. The use of game theory to measure the vulnerability of stochastic networks. IEEE Trans Rel 2003;52(1):63–8.
[3] Zhang X, Mahadevan S. A game theoretic approach to network reliability assessment. IEEE Trans Rel 2017;66(3):875–92.

[4] Fang Y, Sansavini G. Optimizing power system investments and resilience against attacks. Reliab Eng Sys Saf 2017;159:161–73.
[5] Ding T, Yao L, Li F. A multi-uncertainty-set based two-stage robust optimization to defender–attacker–defender model for power system protection. Reliab Eng Sys Saf 2018;169:179–86.
[6] Chen L, Miller-Hooks E. Resilience: an indicator of recovery capability in intermodal freight transport. Transp Sci 2012;46(1):109–21.
[7] Barker K, Ramirez-Marquez JE, Rocco CM. Resilience-based network component importance measures. Reliab Eng Syst Saf 2013;117:89–97.
[8] Fotouhi H, Moryadee S, Miller-Hooks E. Quantifying the resilience of an urban traffic-electric power coupled system. Reliab Eng Syst Saf 2017;163:79–94.
[9] Zio E. Challenges in the vulnerability and risk analysis of critical infrastructures. Reliab Eng Syst Saf 2016;152:137–50.
[10] Zhang X, Mahadevan S, Sankararaman S, Goebel K. Resilience-based network design under uncertainty. Reliab Eng Syst Saf 2018;169:364–79.
[11] Woods D. Four concepts for resilience and the implications for the future of resilience engineering. Reliab Eng Syst Saf 2015;141:5–9.
[12] Toumazis I, Kwon C. Routing hazardous materials on time-dependent networks using conditional value-at-risk. Transp Res Part C 2013;37:73–92.
[13] Erkut E, Ingolfsson A. Catastrophe avoidance models for hazardous materials route planning. Transp Sci 2000;34(2):165–79.
[14] Kang Y, Batta R, Kwon C. Value-at-Risk model for hazardous material transportation. Ann Oper Res 2014;222:361–87.
[15] Ouyang M. Review on modeling and simulation of interdependent critical infrastructure systems. Reliab Eng Syst Saf 2014;121:43–60.
[16] Johansson J, Hassel H, Zio E. Reliability and vulnerability analyses of critical infrastructures: Comparing two approaches in the context of power systems. Reliab Eng Syst Saf 2013;120:27–38.
[17] Wang J, Kang Y, Kwon C, Batta R. Dual toll pricing for hazardous materials transport with linear delay. Netw Spat Econ 2012;12:147–65.
[18] Adjetey-Bahun K, Birregah B, Châtelet E, Planchet JL. A model to quantify the resilience of mass railway transportation systems. Reliab Eng Syst Saf 2016;153:1–14.
[19] Nogal M, O'Connor A, Caulfield B, Martinez-Pastor B. Resilience of traffic networks: From perturbation to recovery via a dynamic restricted equilibrium model. Reliab Eng Syst Saf 2016;156:84–96.
[20] Chiou SW. A risk-averse signal setting policy for regulating hazardous material transportation under uncertain travel demand. Transp Res Part D 2017;50:446–72.
[21] Ukkusuri S, Ramadurai G, Patil G. A robust transportation signal control problem accounting for traffic dynamics. Comp Oper Res 2010;37:869–79.
[22] Zhang L, Yin Y, Lou Y. Robust signal timing for arterials under day-to-day demand variations. J Transp Res Board 2010;2192:156–66.
[23] Tong Y, Zhao L, Li L, Zhang Y. Stochastic programming model for oversaturated intersection signal timing. Transp Res Part C 2015;58:474–86.
[24] Yin Y. Robust optimal traffic signal timing. Transp Res Part B 2008;42:911–24.
[25] Li JQ. Discretization modeling, integer programming formulations and dynamic programming algorithms for robust traffic signal timing. Transp Res Part C 2011;19:708–19.
[26] Dafermos S. Traffic equilibrium and variational inequalities. Transp Sci 1980;14(1):42–54.
[27] Smith MJ. The existence, uniqueness and stability of traffic equilibria. Transp Res Part B 1979;13(4):295–304.
[28] Chiou SW. TRANSYT derivatives for area traffic control optimisation with network equilibrium flows. Transp Res Part B 2003;37:263–90.
[29] Allsop RE, Charlesworth JA. Traffic in a signal-controlled road network: an example of different signal timings inducing different routeings. Traff Eng Contr 1977;18:262–4.
[30] Suwansirikul C, Friesz TL, Tobin RL. Equilibrium decomposed optimization: a heuristic for continuous equilibrium network design problem. Transp Sci 1987;21:254–63.
[31] Ferrario E, Pedroni N, Zio E. Evaluation of the robustness of critical infrastructures by Hierarchical Graph representation, clustering and Monte Carlo simulation. Reliab Eng Syst Saf 2016;155:78–96.
[32] Chiou SW. Robust stochastic design of signal-controlled road network under uncertain travel demands. IEEE trans Auto Conl 2017;62(7):3152–64.
[33] Varaiya P. Max pressure control of a network of signalized intersections. Transp Res Part C 2013;36:177–95.
[34] Clarke FH. Optimization and nonsmooth analysis. New York: John Wiley; 1983.